Journal of The Electrochemical Society, **157** (7) A753-A759 (2010)
0013-4651/2010/157(7)/A753/7/$28.00 © The Electrochemical Society

Capacitive Manganese Oxide Thin Films Deposited by Reactive Direct Current Sputtering

Chuen-Chang Lin[*,z] **and Peng-Yu Lin**

Department of Chemical and Materials Engineering, National Yunlin University of Science and Technology, Yunlin 64002, Taiwan

Manganese oxide thin films are deposited on graphite foils by a simpler one-step reactive dc sputtering dry process with different volume flow rates of oxygen, sputtering time, pressure, and power. Maximum mass specific capacitance of 344 F/g is obtained in 0.5 M LiCl as well as with optimum sputtering conditions (volume flow rate of oxygen = 10 sccm, sputtering pressure = 20 mTorr, sputtering power = 60 W, and sputtering time = 60 min), and this demonstrates its good mass specific capacitance at a higher sweep rate of 100 mV/s. Furthermore, the geometric specific capacitance increases with increasing sputtering pressure, power, and time. Moreover, the electrochemical stability of the electrode decreases with increasing sputtering pressure.
 [DOI: 10.1149/1.3414823]

Manuscript submitted January 19, 2010; revised manuscript received February 26, 2010. Published May 5, 2010.

Electrochemical capacitors are charge-storage devices which possess a higher power density and a longer cycle life than batteries.[1-3] Their applications include stop/go power sources for hybrid vehicles, starting power for fuel cells, and burst-power generation in electronic devices, etc.[4-9] Electrochemical capacitors are classified into two types, electric double-layer capacitors (EDLC) and pseudocapacitors according to their energy-storage mechanisms. The capacitance of an EDLC arises from the separation of charge at the interface between the electrolyte and the electrode with a high surface area inert material such as activated carbon.[9,10] By contrast, pseudocapacitance arises from fast and reversible redox reactions of electroactive materials with several oxidation states.[1,9-15]

Ruthenium is not suitable for a wider commercialization due to being relatively expensive. Hence, the more economical manganese oxide with a variety of stable valence states appears to be a substitute electrode material for electrochemical capacitors. Therefore, manganese oxides were prepared by different wet processes for their application as electrode materials in electrochemical capacitors.[10,16-18] For example, colloidal manganese oxide was prepared by reducing $KMnO_4$ with $MnCl_2$. The sol–gel-derived nanoparticulate MnO_2 thin film then formed on nickel foils by dip-coating exhibits a high mass specific capacitance of 698 F/g and long cycle life. However, it is a two-step process and the discharge time achieved is only about 1.1 s at a constant current of 0.1 mA due to the MnO_2 thin film.[18] However, some residual impurities could be carried over from these wet processes, and these might affect electrochemical properties (such as conductance) of electrodes. Therefore, a simpler one-step reactive dc sputtering dry process was applied to deposit manganese oxide films on graphite foils in this research. Mn films were deposited by sputtering and then manganese oxide films were synthesized by anodic oxidation; the mass specific capacitance of the films yielded 400–450 F/g at a potential scan rate of 5 mV/s.[9] Increasing the thickness of the dense Mn layer fabricated in a sputter deposition system results in increasing the thickness of the porous Mn oxide surface layer produced during the electrochemical oxidation, but with a constant amount of hydration and little change in the mass specific capacitance.[19] The electrochemical oxidation of the Mn layer fabricated in a sputter deposition system occurs through the following sequence of hydrated oxides: Mn to MnO to Mn_3O_4 to Mn_2O_3 to MnO_2.[20] In earlier work, a ruthenium oxide thin film was deposited on a Pt/Ti/Si substrate by a specially designed dc reactive sputtering method: The capacitance per volume of the thin-film supercapacitor at the first cycle was 38 mF/cm^2 μm.[21]

Contamination, the roughness of the substrate, film thickness, some sputtering parameters (such as sputtering pressure, substrate temperature and bias voltage), etc., have an effect on adhesion,[22-27] which influences operational stability of electrochemical capacitors. Enhanced adhesion was observed at a lower sputtering pressure and for thicker films with rough surfaces.[22] Sputter cleaning seemed to be one of the most effective methods in the physical vapor deposition process to improve adhesion and sputter cleaning with argon showed the best adhesion after 30 min of argon bombardment by simple mechanical test,[23] thus, sputter cleaning with argon for 30 min was applied for the substrate in this paper. In earlier work, ruthenium oxide films were deposited on Si and Ti substrates by reactive radio-frequency magnetron sputtering and the total anodic voltammetric charges increased with an increasing roughness factor.[28] Because the highly rough surface should possess the high surface area, the mass specific capacitance also increased with increasing the roughness factor for manganese oxide.[29] Furthermore, the sputtering yield is reduced so that the deposition rate is reduced also when the oxygen concentration in the sputtering gas (argon and oxygen) is increased, because metal–oxygen reaction occurs on the target surface.[30] Thus, the oxygen concentration changes the surface roughness, crystallization, and oxidation state, which influence specific capacitance and operational stability of electrochemical capacitors. Moreover, sputtering also offers the opportunity to control structural (such as surface roughness and crystallization) and stoichiometric (oxidation state) development of mixing metal–oxygen materials.

This paper examines the effects of sputtering conditions (pressure, power, time, and volume flow rates of oxygen) on specific capacitance and sputtering pressure as well as time on the operational stability of electrochemical capacitors.

Experimental

A graphite foil was used as a substrate due to its lower specific resistance (lower than that of activated carbon and silicon).[31] In mechanical polishing, the graphite foil (1×1 or 1×2 cm^2) was abraded with SiC paper and then rinsed ultrasonically with deionized water for 10 min. To increase its surface roughness, for the chemical acid wash, it was then etched in 6 M aqueous HCl at room temperature for 30 min and subsequently rinsed ultrasonically with deionized water for 10 min. Next, it was degreased ultrasonically in acetone until any surface grease was completely eliminated, rinsed with pure deionized water, and subsequently oven-dried in air (50°C) to constant weight. Finally, sputter cleaning with argon for 30 min was applied for the substrate and then it was reweighed for sputtering.

The manganese oxide film was deposited on the pretreated and grounded graphite foil substrate by reactive dc magnetron sputtering from a 3 in. disk Mn (purity: 99.9%, melting point: about 535°C, purchased from SCM, INC) target in a vacuum chamber with a background pressure of 7×10^{-6} Torr. The distance between the target and the substrate was 8 cm. During deposition, the substrate

* Electrochemical Society Active Member.
[z] E-mail: linchuen@yuntech.edu.tw

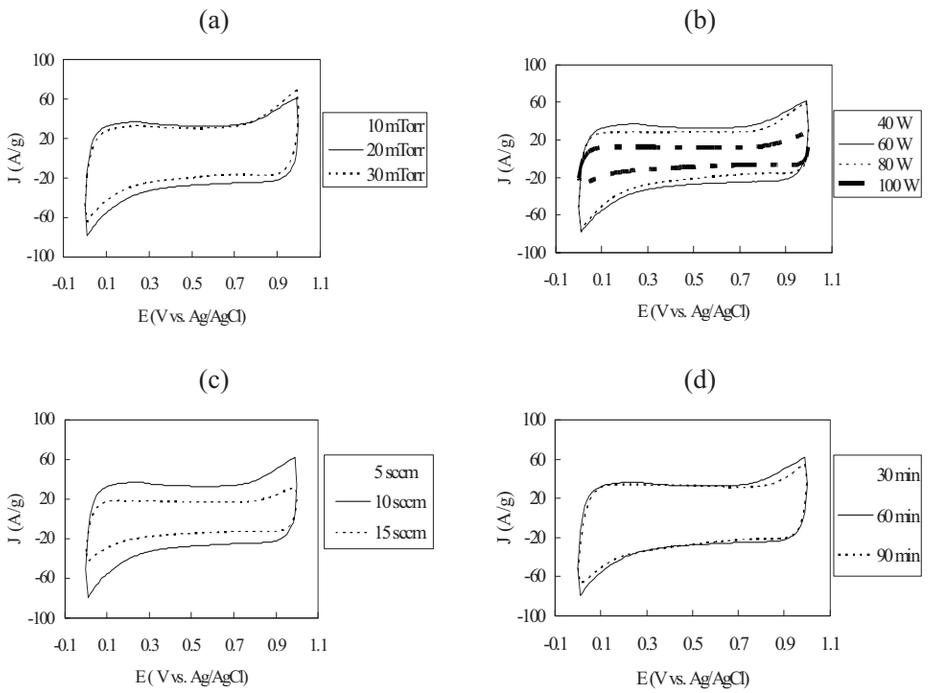

Figure 1. CVs (the 100th charge–discharge cycle) at a potential scan rate of 100 mV/s for the manganese oxide electrode prepared at (a) different pressure (with optimum sputtering conditions: 60 min, 10 sccm oxygen, and 60 W), (b) different sputtering power (with optimum sputtering conditions: 60 min, 10 sccm oxygen, and 20 mTorr), (c) different volume flow rates of oxygen (with optimum sputtering conditions: 60 min, 20 mTorr, and 60 W), and (d) different sputtering time (with optimum sputtering conditions: 10 sccm oxygen, 20 mTorr, and 60 W).

(about 55°C) was not intentionally heated. The volume flow rate of argon was maintained at 25 sccm. The volume flow rates (5, 10, and 15 sccm) of oxygen were varied, sputtering pressure (10, 20, and 30 mTorr) was varied, sputtering power (40, 60, 80, and 100 W) was varied, and sputtering time (30, 60, and 90 min) was also varied. Finally, the graphite foil with manganese oxide thin films was weighed to five decimals (0.00001 g) and thus the mass of the film could be determined with the small percentage errors.

The electrochemical measurements for the prepared graphite foil electrodes were performed by an electrochemical analyzer (CH Instruments CHI 608B, U.S.). The three-electrode cell consisted of Ag/AgCl as the reference electrode, Pt as the counter electrode and the prepared electrode as the working electrode. The electrolytes were degassed with purified nitrogen gas before voltammetric measurements, and nitrogen was passed over the solution during all the measurements. The solution temperature was maintained at 25°C by means of a circulating water thermostat (HAAKE DC3 and K20, Germany). The cyclic voltammogram (CV) was taken with the potential scan rate (100 mV/s) and a 0.5 M aqueous electrolyte (LiCl, pH = 6.7). The potential window in the range of 0–1 V was used in all measurements except where stated. Capacitance is normalized to 1 g of manganese oxide.

Surface morphology of the electrodes prepared at different conditions was conducted by a field-emission-scanning electron microscope (JEOL JSM-6700F, Japan). In addition, the chemical environment of the manganese oxide film deposited on the graphite foil with the different volume flow rates of oxygen and the electrode (using optimum sputtering conditions: 10 sccm oxygen, 60 min, 20 mTorr, and 60 W) before as well as after the potential cycling was explored by an X-ray photoemission spectroscope (XPS, Fison VG. ESCA210, England). Furthermore, additional information on the surface roughness of the electrodes prepared at different conditions was obtained by atomic force microscope (AFM, Digital Instrument NanoMan NS4 + D3100, U.S.). Moreover, X-ray diffraction (XRD, MAC SCIENCE, Japan) with a low angle of incidence was used to characterize the crystalline structure of the graphite foil and the manganese oxide film deposited on the graphite foil using optimum sputtering conditions.

Results and Discussion

CVs at a potential scan rate of 100 mV/s for the manganese oxide electrode prepared at (a) different pressure, (b) different sputtering power, (c) different volume flow rates of oxygen, and (d) different sputtering time are shown in Fig. 1. All CVs in Fig. 1 for the manganese oxide electrode prepared at different sputtering conditions are similar (no evidently observable redox peaks) and show a mirror image with respect to the zero-current line and a rapid current response on voltage reversal at potentials near the two limits of the potential window. These features indicate that hydrated cations (such as Li^+ and proton) of the electrolyte (pH = 6.7) have a rapid chemisorption/desorption reaction rate and are involved in the charge-storage process within the very near surface thin layer of manganese oxide electrodes.[32,33] Electrochemical quartz-crystal microbalance as well as X-ray photoelectron spectroscopy data further indicate that proton plays the predominant role and the charge–discharge reaction in the LiCl solution can be expressed as: $Mn(IV)O_2 + 0.767\lambda H^+ + 0.233\lambda Li^+ + \lambda e^- \Leftrightarrow H^+_{0.767\lambda}Li^+_{0.233\lambda}[Mn(III)_\lambda Mn(IV)_{1-\lambda}]O_2$.[34] In addition, the capacitance of the pure graphite foil (1×2 cm^2) is 0.00216 F, which is about 6.27% of the total capacitance of the manganese oxide electrode using optimum sputtering conditions. Therefore, if there is some contribution to the total capacitance of the manganese oxide electrode from the graphite foil which manganese oxide thin films were sputtered on, it seems unimportant.

Figure 2 shows the effects of the sputtering pressure on the mass specific capacitance. The mass specific capacitance reached a maximum at 20 mTorr of sputtering pressure. The mass specific capacitance increased at the range from 10 to 20 mTorr of sputter ing pressure. This picture may be explained as follows. A higher sputtering pressure leads to higher collision frequencies [$Z = (\pi d^2 C_{rel} P)/(kT)$, where Z is the collision frequency, d is the average diameter of particles, C_{rel} is the relative mean speed, P is pressure, k is Boltzmann's constant, and T is temperature] and a lower kinetic energy. A lower kinetic energy leads to the lower mobility on the surface of the substrate for particles (Mn atoms or MnO "clusters"). This would cause a higher surface roughness (see Fig. 3,

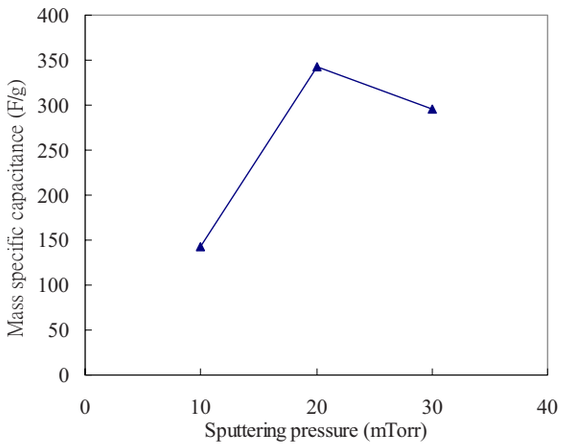

Figure 2. (Color online) The effects of sputtering pressure on the mass specific capacitance (with optimum sputtering conditions: 60 min, 10 sccm oxygen, and 60 W).

i.e., there is an increase in the height of the surviving particles in a particle-migration coalescence process), thus leading to a higher mass specific capacitance (a similar result has been published in previously[28,29]). However, mass specific capacitance decreased at a sputtering pressure in the range 20–30 mTorr. This picture may be attributed to a too high sputtering pressure, leading to too many particles, and thus causing a shadowing effect which enhances many collision probability, and so declining much kinetic energy/mobility on the surface of the substrate for particles. This leads to a decreasing surface roughness (see Fig. 3) and mass specific capacitance.

Figure 4 shows the effects of sputtering power on the mass specific capacitance. The mass specific capacitance reached a maximum at 60 W. The mass specific capacitance increased at sputtering power in the range 40–60 W. This illustrates that the higher the sputtering power, the higher the sputtering yield, thus enhancing the deposition rate. Then particles falling on the substrate do not have enough time to rearrange and resputter themselves, which leads to increasing surface roughness (see Fig. 5), and so leading to a higher mass specific capacitance. However, the mass specific capacitance decreased with sputtering power in the range 60–100 W. This picture may be attributed to a too high sputtering power, leading to a too strong ion as well as reflected neutral bombardment of the substrate surface, then only causing more damages, thus decreasing surface roughness (see Fig. 5) and mass specific capacitance.

Figure 6 shows the effects of different volume flow rates of oxygen on the mass specific capacitance. The mass specific capacitance reached the maximum at 10 sccm oxygen. The mass specific capacitance increased in the range 5–10 sccm of oxygen. The reason behind this behavior may be that at higher volume flow rates of oxygen, the more oxygen ions would lead to a greater oxygen ion bombardment of the substrate surface due to a sheath voltage (the difference between the plasma potential and the substrate potential), enhancing surface roughness (see Fig. 7), and finally increasing the mass specific capacitance. However, the mass specific capacitance decreased in the range 10–15 sccm of oxygen. This may indicate that with a too high volume flow rate of oxygen, too many oxygen ions would cause a shadowing effect which prevented argon ions from bombarding the target and even lead to lighter oxygen ions (as opposed to heavier argon ions) bombarding the target because of the sheath voltage as well as oxide formation on the target. Thus the sputtering yield is reduced so that the deposition rate drops. Consequently, particles falling on the substrate have sufficient time to rearrange and resputter themselves, which leads to decreasing surface roughness (see Fig. 7) and mass specific capacitance. To investigate the chemical environment of manganese oxide on the graphite foil electrode, XPS was used to examine the binding energy of manganese oxide thin films sputtered with optimum sputtering pressure

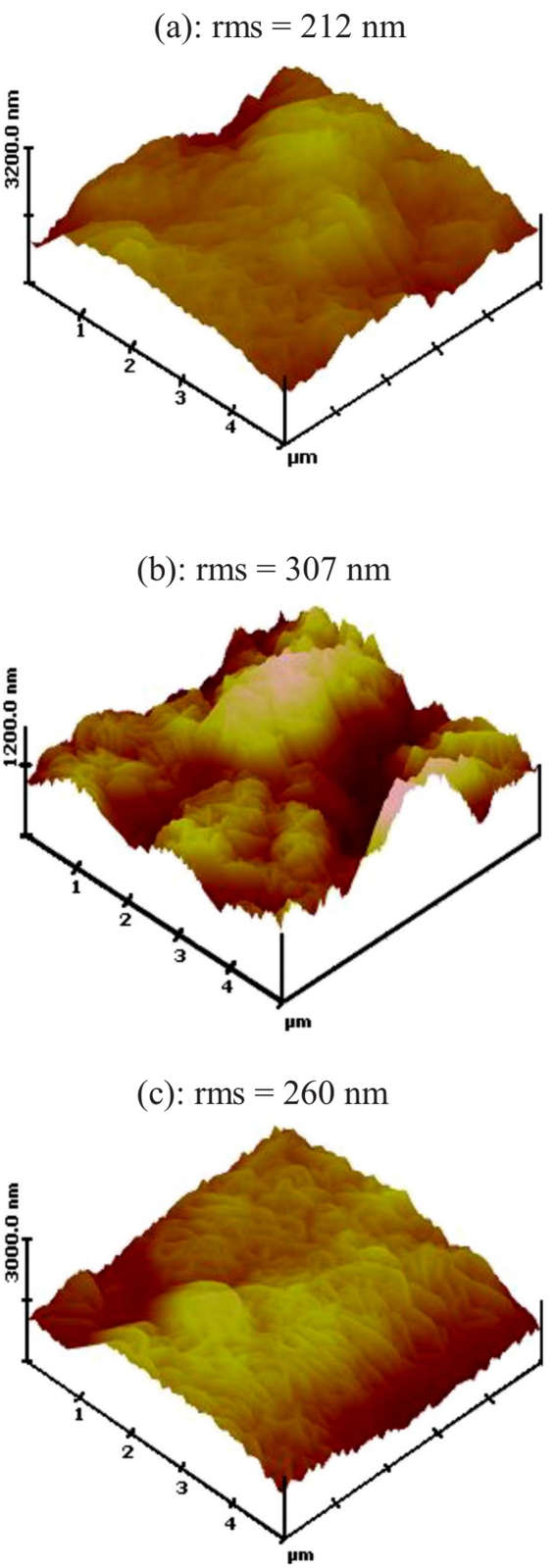

Figure 3. (Color online) AFM micrograph [(a) 10, (b) 20, and (c) 30 mTorr] of the electrode prepared at different pressure (with optimum sputtering conditions: 60 min, 10 sccm oxygen, and 60 W).

(20 mTorr), power (60 W), as well as time (60 min) and different volume flow rates of oxygen. XPS spectral data of Mn $2p_{3/2}$ and

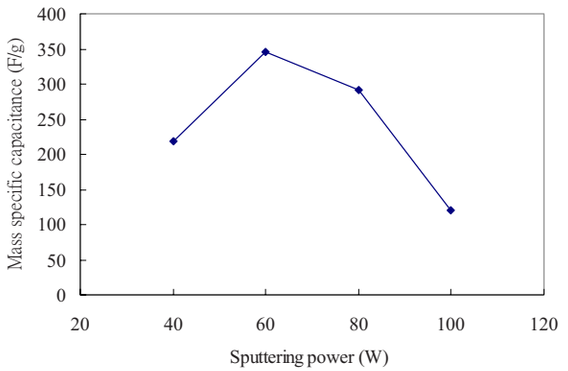

Figure 4. (Color online) The effects of sputtering power on the mass specific capacitance (with optimum sputtering conditions: 60 min, 10 sccm oxygen, and 20 mTorr).

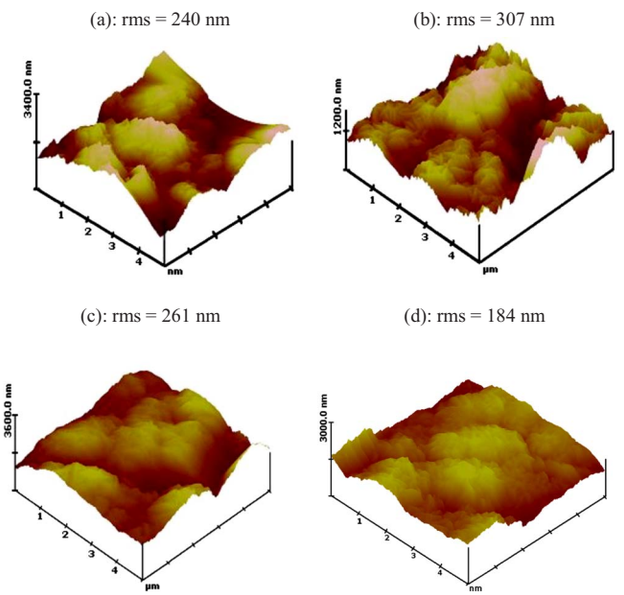

Figure 5. (Color online) AFM micrograph [(a) 40, (b) 60, (c) 80, and (d) 100 W] of the electrode prepared at different sputtering power (with optimum sputtering conditions: 60 min, 10 sccm oxygen, and 20 mTorr).

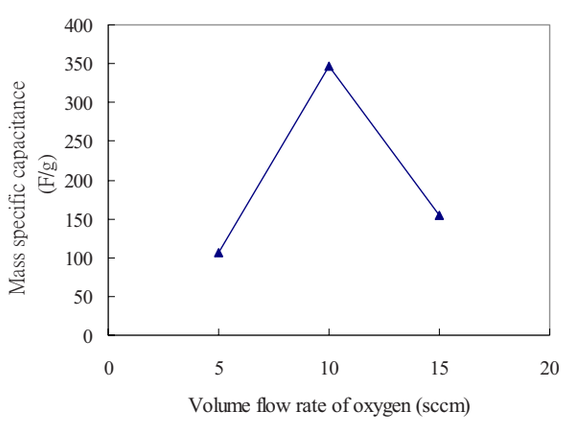

Figure 6. (Color online) The effects of different volume flow rates of oxygen on the mass specific capacitance (with optimum sputtering conditions: 60 min, 20 mTorr, and 60 W).

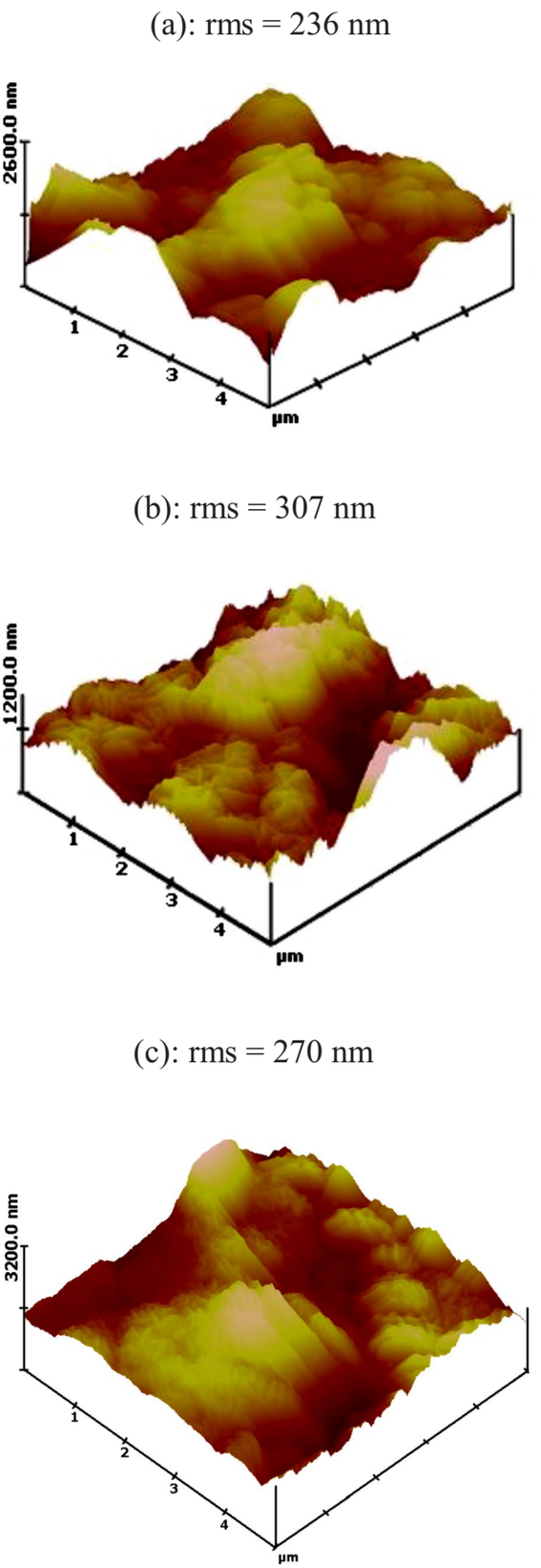

Figure 7. (Color online) AFM micrograph [(a) 5, (b) 10, and (c) 15 sccm] of the electrode prepared at different volume flow rates of oxygen (with optimum sputtering conditions: 60 min, 20 mTorr, and 60 W).

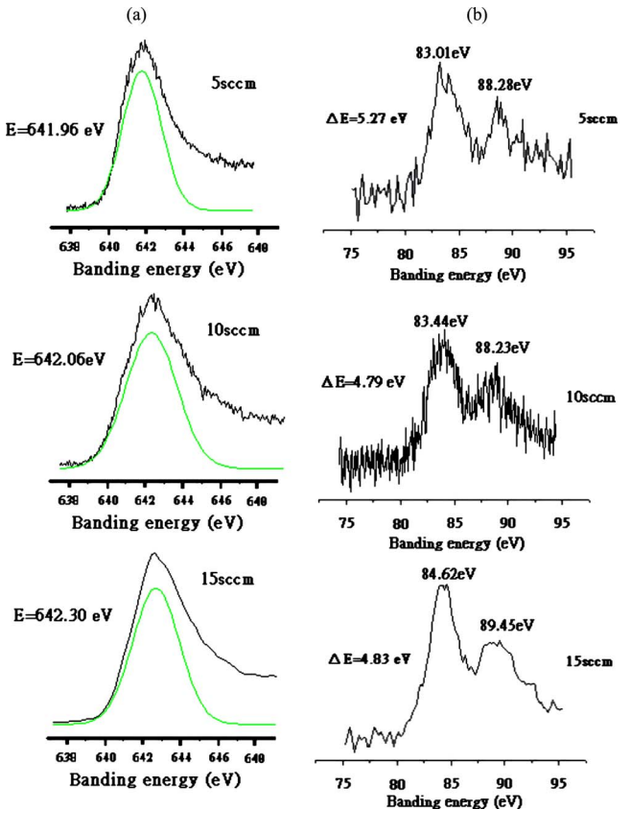

Figure 8. (Color online) XPS spectral data of (a) Mn $2p_{3/2}$ and (b) Mn 3s for manganese oxide sputtered with optimum dc sputtering pressure (20 mTorr), power (60 W), as well as time (60 min) and different volume flow rates of oxygen.

Mn 3s (see Fig. 8) for manganese oxide thin films sputtered with different volume flow rates of oxygen are listed in Table I. For Mn $2p_{3/2}$, binding energy for manganese oxide increased from 641.96 to 642.06 and 642.30 eV following 10 and 15 sccm oxygen, respectively. These results show that the oxidation state of manganese oxide increased after increasing the volume flow rate of oxygen from 5 to 10 or 15 sccm oxygen. The oxidation state of manganese oxide was also determined by the differences in binding energies between the splitting peaks of Mn 3s in Table I. The difference in the binding energy for manganese oxide changed from 5.27 to 4.79 eV and 4.83 eV following 10 and 15 sccm oxygen, respectively. Thus, manganese oxide thin films sputtered with 5 sccm oxygen mainly consist of Mn^{3+} species and manganese oxide thin films sputtered with 10 or 15 sccm oxygen almost consisted of Mn^{4+} species.[33,35] Therefore, at volume flow rates of oxygen in the range 5–10 sccm, the higher the volume flow rates of oxygen, the larger

Table I. XPS Mn $2p_{3/2}$ and Mn 3s binding energies (eV) and differences of binding energies (eV) for manganese oxide sputtered with optimum dc sputtering pressure (20 mTorr), power (60 W), as well as time (60 min) and different volume flow rates of oxygen.

	Mn $2p_{3/2}$	Mn 3s		
Volume flow rates of oxygen (sccm)	Eb (eV)	Eb(1) (eV)	Eb(2) (eV)	ΔE (eV)
5	641.96	83.01	88.28	5.27
10	642.06	83.44	88.23	4.79
15	642.30	84.62	89.45	4.83

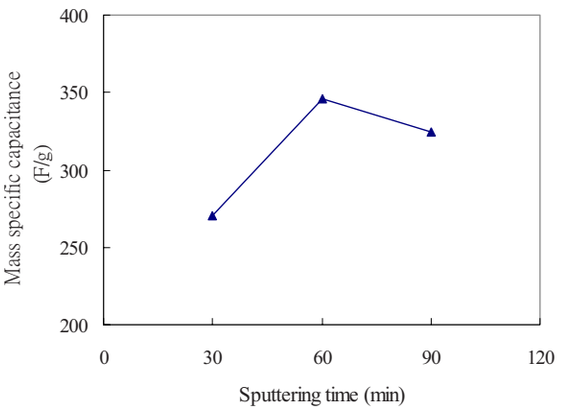

Figure 9. (Color online) The effects of sputtering time on the mass specific capacitance (with optimum sputtering conditions: 10 sccm oxygen, 20 mTorr, and 60 W).

the amount of trivalent manganese oxide as well as the higher the surface roughness, and the higher the mass specific capacitance (see Table I and Fig. 6 and 7). A similar result has been published previously.[3,28,29] However, at volume flow rates of oxygen in the range 10–15 sccm, the amounts of trivalent manganese oxide were almost the same due to the excess oxygen, and the mass specific capacitance decreased because of decreasing surface roughness (see Table I and Fig. 6 and 7).

Figure 9 shows the effects of sputtering time on the mass specific capacitance. The mass specific capacitance reached a maximum at 60 min. The mass specific capacitance increased with sputtering time in the range 30–60 min. This picture may be that a higher sputtering time led to a higher surface roughness (see Fig. 10), thus leading to a higher mass specific capacitance. However, the mass specific capacitance decreased for sputtering times in the range 60–90 min. This may indicate that higher sputtering times lead to a lower surface roughness (see Fig. 10), and thus to a lower mass specific capacitance. Furthermore, Fig. 11 shows the effects of sputtering time and different charge–discharge cycles on the mass specific capacitance of the electrode (fabricated by optimum sputtering conditions: 10 sccm oxygen, 20 mTorr, and 60 W). The mass specific capacitance of the electrode increased gradually with increasing number of charge–discharge cycles during the first 600 cycles of potential cycling. The reason behind this behavior may be that at more potential cycles, the percentage of incorporated water may increase from the electrolyte (the 0th cycle of potential cycles: 19.20 atom % incorporated water, and the 100th cycle of potential cycles: 26.20 atom % incorporated water). This causes a higher mass specific capacitance because the combined water (incorporated water and free water from the electrolyte) promotes the movement of the protons in the solid phase,[18] and thus electrolyte ions more easily diffuse into the inner pores of the electrodes and consequently some potentially electroactive sites on the inner pores are able to contribute to the mass specific capacitance with higher levels of combined water.

XRD patterns of the freshly polished graphite foil and the electrode fabricated by optimum sputtering conditions (volume flow rate of oxygen = 10 sccm, sputtering pressure = 20 mTorr, sputtering power = 60 W, and sputtering time = 60 min) are shown in Fig. 12. The peaks in Fig. 12a are identified as coming from carbon crystals. The major peaks in Fig. 12b is the same as those in Fig. 12a except for the very low intensity peak from the MnO_2 (2θ = 37.237 from JCPDS) crystals in Fig. 12b due to a thin film of poorly crystalline MnO_2 deposited on the graphite foil.

The structure of the sputtered films depends on the substrate temperature/target melting point and inert sputtering gas pressure.[27] The substrate temperature (about 55°C)/target melting point (about

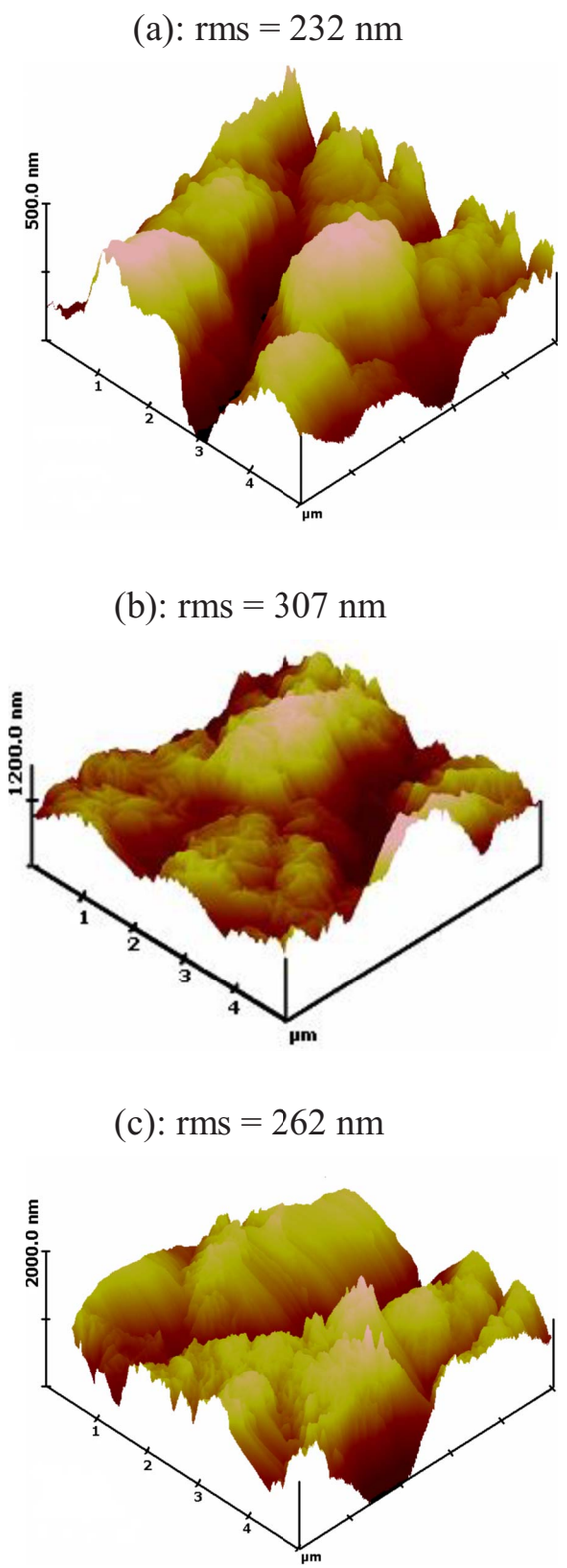

Figure 10. (Color online) AFM micrograph [(a) 30, (b) 60, and (c) 90 min] of the electrode prepared at different sputtering time (with optimum sputtering conditions: 10 sccm oxygen, 20 mTorr, and 60 W).

535°C) is about 0.1 and the inert sputtering gas pressure is about 0.83–3.34 Pa calculated from the volume flow rate (25 sccm) of argon, volume flow rates (5, 10, and 15 sccm) of oxygen, and sputtering pressure (10, 20, and 30 mTorr) in this research. Therefore, according to the similar zone scheme (structure zone model) introduced by Thornton with four zones (1, T, 2, 3), the manganese oxide film on the pretreated graphite foil (substrate) belongs to the zone 1 structure (voided boundaries and fibrous grains), which appears in amorphous and crystalline deposits, is the result of shadowing effects which overcome limited adatom surface diffusion.[27] In addition, sputtering pressure affects film microstructure through several indirect mechanisms. For example, if sputtering pressure is increased to the point where the mean free path for elastic collisions between the sputtered atoms and sputtering gas becomes of the order of the target-substrate distance, the oblique component of the deposition flux is increased because of gas scattering. This results in a more open zone 1 structure.[27] Moreover, the roughness and temperature of the substrate affect the growth of the manganese oxide film.[27] To increase surface roughness of the graphite foil, it was then etched in aqueous HCl and thus zone 1 was promoted by the roughness and low temperature (about 55°C) of the substrate in this study.

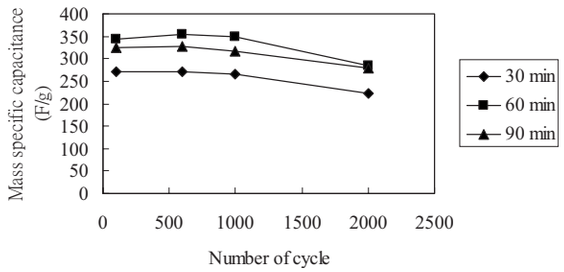

Figure 11. The effects of sputtering time and different charge–discharge cycles on the mass specific capacitance of the electrode (fabricated by optimum sputtering conditions: 10 sccm oxygen, 20 mTorr, and 60 W).

Conclusions

A dc magnetron sputtering dry process was employed to deposit manganese oxide onto graphite foil. Maximum mass specific capacitance of 344 F/g was obtained with optimum sputtering conditions. Furthermore, the mass specific capacitance increased at a lower sputtering pressure/volume flow rates of oxygen, but decreased at a higher sputtering pressure/volume flow rates of oxygen due to a shadowing effect. The mass specific capacitance increased at a lower sputtering power, but decreased at a higher sputtering power because of a too strong ion and reflected neutral bombardment. Moreover, the higher the volume flow rates of oxygen, the larger the amount of trivalent manganese oxide and the higher the surface roughness, the higher the mass specific capacitance at volume flow rates of oxygen in the range 5–10 sccm, but the amounts of trivalent manganese oxide were almost the same and the mass specific capacitance decreased at volume flow rates of oxygen in the range 10–15 sccm.

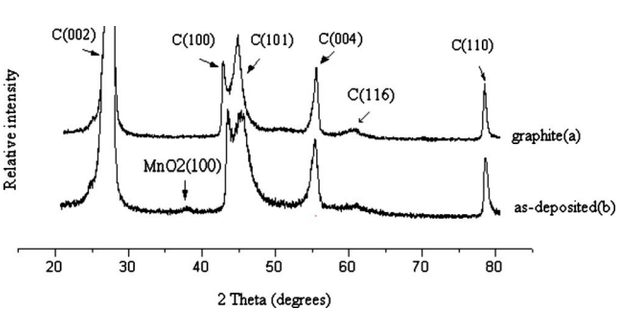

Figure 12. (Color online) XRD patterns of the freshly polished graphite foil and the electrode fabricated by optimum sputtering conditions (volume flow rate of oxygen = 10 sccm, sputtering pressure = 20 mTorr, sputtering power = 60 W, and sputtering time = 60 min).

National Yunlin University of Science and Technology assisted in meeting the publication costs of this article.

References

1. B. E. Conway, *Electrochemical Supercapacitors: Scientific Fundamentals and Technological Applications*, Kluwer Academic/Plenum Publishers, New York (1999).
2. R. Kötz and M. Carlen, *Electrochim. Acta*, **45**, 2483 (2000).
3. J. K. Chang and W. T. Tsai, *J. Electrochem. Soc.*, **150**, A1333 (2003).
4. Y. S. Chen and C. C. Hu, *Electrochem. Solid-State Lett.*, **6**, A210 (2003).
5. Y. U. Jeong and A. Manthiram, *J. Electrochem. Soc.*, **149**, A1419 (2002).
6. C. C. Hu and C. C. Wang, *J. Electrochem. Soc.*, **150**, A1079 (2003).
7. H. P. Park, O. O. Park, K. H. Shin, C. S. Jin, and J. H. Kim, *Electrochem. Solid-State Lett.*, **5**, H7 (2002).
8. R. N. Reddy and R. G. Reddy, *J. Power Sources*, **124**, 330 (2003).
9. J. N. Broughton and M. J. Brett, *Electrochim. Acta*, **49**, 4439 (2004).
10. M. Wu, G. A. Snook, G. Z. Chen, and D. J. Fray, *Electrochem. Commun.*, **6**, 499 (2004).
11. A. Burke, *J. Power Sources*, **91**, 37 (2000).
12. J. K. Chang and W. T. Tsai, *Electrochem. Commun.*, **6**, 666 (2004).
13. M. S. Hong, S. H. Lee, and S. W. Kim, *Electrochem. Solid-State Lett.*, **5**, A227 (2002).
14. J. H. Park, J. M. Ko, and O. O. Park, *J. Electrochem. Soc.*, **150**, A864 (2003).
15. J. R. Zhang, B. Chen, W. K. Li, J. J. Zhu, and L. P. Jiang, *Int. J. Mod. Phys. B*, **16**, 4479 (2002).
16. C. C. Lin and C. C. Yen, *J. Appl. Electrochem.*, **38**, 1677 (2008).
17. C. C. Lin and H. W. Chen, *Electrochim. Acta*, **54**, 3073 (2009).
18. S. C. Pang, M. A. Anderson, and W. C. Thomas, *J. Electrochem. Soc.*, **147**, 444 (2000).
19. B. Djurfors, J. N. Broughton, M. J. Brett, and D. G. Ivey, *J. Power Sources*, **156**, 741 (2006).
20. B. Djurfors, J. N. Broughton, M. J. Brett, and D. G. Ivey, *J. Electrochem. Soc.*, **153**, A64 (2006).
21. J. H. Lim, D. J. Choi, H. K. Kim, W. H. Cho, and Y. S. Yoon, *J. Electrochem. Soc.*, **148**, A275 (2001).
22. L. P. Ward and P. K. Datta, *Thin Solid Films*, **271**, 101 (1995).
23. K. Koski, J. Holsa, J. Ernoult, and A. Rouzaud, *Surf. Coat. Technol.*, **80**, 195 (1996).
24. G. Reiners and M. Griepentrog, *Surf. Coat. Technol.*, **76–77**, 809 (1995).
25. H. Liu and X. Zhang, *Thin Solid Films*, **240**, 97 (1994).
26. X. Wang, G. Yang, X. Liu, Z. Zheng, W. Huang, and S. Zou, *Mater. Sci. Eng., A*, **156**, 91 (1992).
27. M. Ohring, *Materials Science of Thin Films*, Academic, New York (2002).
28. G. Battaglin, V. Rigato, S. Zandolin, A. Benedetti, S. Ferro, L. Nanni, and A. De Battisti, *Chem. Mater.*, **16**, 946 (2004).
29. C. C. Hu and T. W. Tsou, *J. Power Sources*, **115**, 179 (2003).
30. J. H. Huang and J. S. Chen, *Thin Solid Films*, **382**, 139 (2001).
31. C. C. Lin and C. C. Yen, *J. Appl. Electrochem.*, **37**, 813 (2007).
32. H. Y. Lee and J. B. Goodenough, *J. Solid State Chem.*, **144**, 220 (1999).
33. M. Toupin, T. Brousse, and D. Bélanger, *Chem. Mater.*, **16**, 3184 (2004).
34. S. L. Kuo and N. L. Wu, *J. Electrochem. Soc.*, **153**, A1317 (2006).
35. M. Chigane and M. Ishikawa, *J. Electrochem. Soc.*, **147**, 2246 (2000).